MICROSCALE CHLORIDE SENSOR

F.Cao,[1] D.W. Greve,[1] I.J. Oppenheim,[2] J. VanBriesen[2]

[1]Department of Electrical and Computer Engineering, Carnegie Mellon University
[2]Department of Civil and Environmental Engineering, Carnegie Mellon University
Pittsburgh, PA 15213 USA

Measurements of chloride concentration are important in a range of applications. We report here on our progress toward the fabrication and testing of small, inexpensive chloride sensors integrated with sensing electronics on a CMOS chip. We describe and demonstrate a process for formation of gold and silver chloride/ silver electrodes on a CMOS chip. Cyclic voltammetry is performed on chip-scale electrodes and the test results are discussed.

I. Introduction

Measurements of chloride concentration are important in a range of applications. These include the detection of chloride infiltration into reinforced concrete and the monitoring of active chlorine concentrations in drinking water. There is therefore interest in integrated sensors that can monitor the chloride concentration at low cost with enough sensitivity and stability.

Previous chloride sensors typically used electrochemical techniques. Researchers have proposed sensors based on half-cell potential technique with silver/silver chloride reference electrodes embedded in concrete (1). A disposable microsensor for monitoring free chlorine in water using microelectrodes with cyclic voltammetry technique was reported in (2). This microsensor still requires an external potentiostat to control the sensor. A CMOS integrated VLSI potentiostatic control circuit was reported in (3), which was tested for cyclic voltammetry with external two-electrode cells. We have recently reported on developing an amperometric sensor based on cyclic voltammetry for chlorine monitoring (4). Here we present our progress toward development of the chloride sensor integrated with both the microelectrodes and potentiostat electronics on a CMOS chip.

II. Sensor Description and Micro-electrode

The sensor integrates an array of three-electrode electrochemical cells with the potentiostat required for voltammetric or amperometric sensing on a CMOS chip. The potentiostat is based on a CMOS operational amplifier and is shown in Fig. 1. The electrode areas are 200 μm × 200 μm (WE, working electrode), 100 μm × 200 μm (CE, counter electrode) and 50 μm × 200 μm (RE, reference electrode). Each sensor,

consisting of electrodes and the associated operational amplifier, occupies only an area of about 0.5 mm × 0.35 mm. This small size makes it possible to fabricate several complete sensing sites in the area of a 2 mm × 2 mm chip.

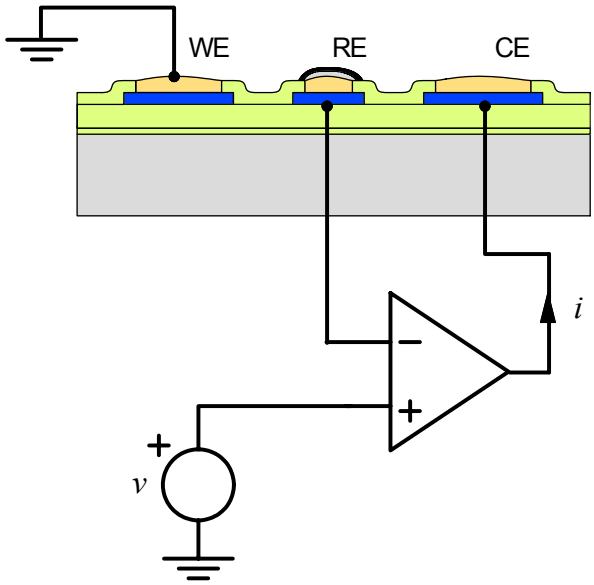

Figure 1. Three-electrode cell with op-amp circuit

There are some additional advantages beyond reduced size for choosing microelectrodes instead of conventional large-scale electrodes. One of the most important is the potential for improved signal to noise ratio for cyclic voltammetry. Cyclic voltammetry measures the faradic current for a voltage scan. As the voltage at the electrode changes, a redox reaction occurs at the electrode and a faradic current is formed. For large electrodes the faradic current is given by

$$i_f = -nFAJ \qquad [1]$$

where n is the number of electrons transferred, F is the Faraday constant, A is the area of the electrode and J is the mass transport flux. As the electrode size decreases, there is an enhanced rate of mass transport at the edges of microelectrodes. Such edge effects result in a higher current density than given by [1].

During the voltage scan there is also a non-faradic current associated with charging and discharging of the double-layer near the electrode. This represents an undesired current not related to the redox reaction and is given by

$$i_c = \frac{dq}{dt} \approx C_{dl} A \frac{dv}{dt} \qquad [2]$$

where dv/dt is the voltage scan rate, and C_{dl} is the double-layer capacitance per unit area. C_{dl} is nearly constant even for small electrodes, because the double layer thickness is around 10 nm, which is much smaller than the electrode size. As the electrode area decreases, the faradic current density increases due to the edge effect while the non-faradic current density remains the same, and as a result the signal-to-background ratio is improved (5).

Another significant advantage for microelectrodes is that the smaller total current makes the IR drop smaller. This allows the microelectrode system to work in a highly resistive environment with little electrolyte support (5).

Finally, a microelectrode has a smaller double-layer capacitance. This allows it to work in a high-speed voltage scan. During cyclic voltammetry, a high voltage scan rate results in a higher peak current response, which also means higher sensitivity.

III. Process Flow

The process flow for the sensor is illustrated in Fig. 2.

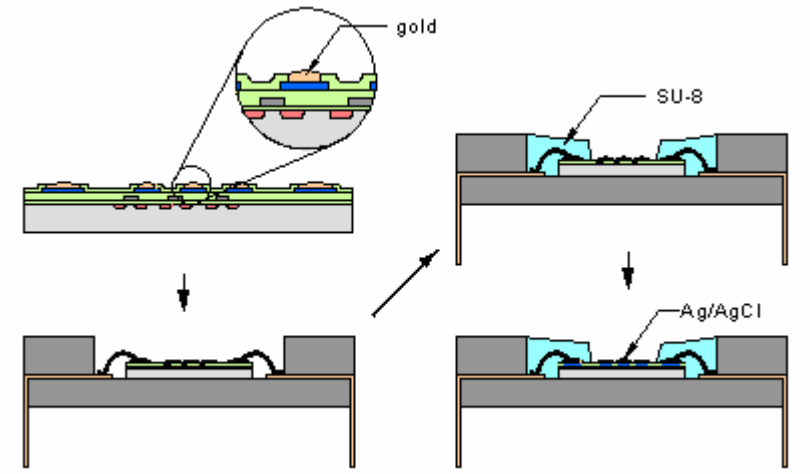

Figure 2. Process steps for fabrication of integrated chloride sensor.

We begin with a CMOS chip fabricated using the AMIS 1.5 micron process available through MOSIS (6). The chip contains operational amplifiers, readout circuitry, plating control circuitry and sensing electrode pads. Electroless gold plating is used to coat all exposed electrode pads with gold. Details of this process have been described in (7) and tested in (8). Briefly, gold plating of the aluminum electrodes requires removal of the surface oxide; activation of the surface by single or double zincation; plating of a thick layer of nickel and finally immersion electroless plating of gold. No external power source is required during this process. The chip is then mounted into a package and wire-bonded, after which the chip cavity and bond wires are covered with SU8-10 photoresist. A coarse photolithographic step then exposes

electrodes at the interior of the chip while leaving the bonding pads and bond wires protected. Finally, AgCl/ Ag reference electrodes are created. Silver is deposited by selective electroplating in an electrolyte consisting of saturated Ag_2SO_4 in 0.5 M H_2SO_4. The sensing electrodes are connected to the negative terminal of the voltage source and a silver wire is connected to the positive terminal, as shown in Fig. 3a. The electroplating current is adjusted to 3 µA for 10 min. Silver is electroplated on top of the gold layer by the half-cell reaction

$$Ag^{+} + e^{-} \rightarrow Ag\,. \qquad [3]$$

From the total charge transferred during the electroplating process, a silver layer approximately 2 µm is expected. After silver layer formation is a chlorination step in a saturated KCl electrolyte. The electrodes are connected to the negative terminal of the voltage source and a platinum wire is connected to the negative terminal, as shown in Fig. 3b. A current of 10 µA is forced to flow from the power source to electrodes for 2 minutes. The half-cell reaction is

$$Ag + Cl^{-} \rightarrow Ag + e^{-} \qquad [4]$$

resulting in an estimated AgCl layer thickness of approximately 3 µm.

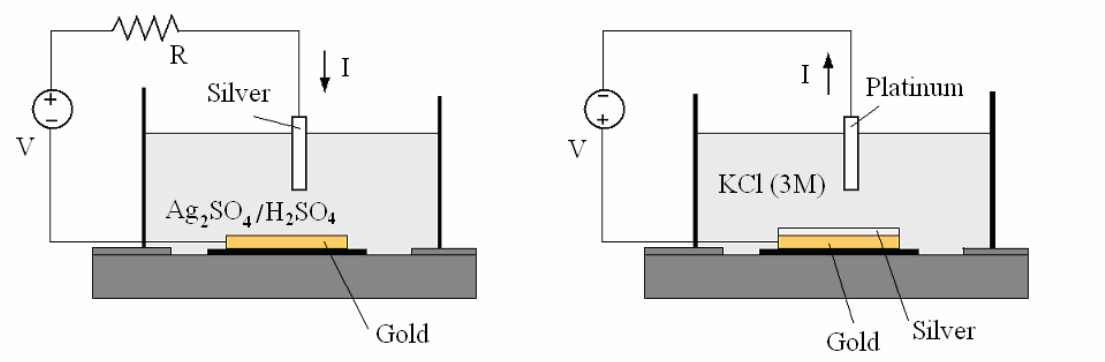

Figure 3. (a) Silver Plating (b) Silver Chloride Formation

IV. Test of Micro-electrode Sensor

Here we report measurements on a test chip with micro-electrodes directly wired to the bond pads. Cyclic voltammetry was performed using an external operational amplifier circuit. In this case the working electrode size is 100 µm × 200 µm and 50 µm × 200 µm electrodes were used for both counter and reference electrodes. All post-process steps described above were performed including formation of the AgCl/ Ag reference electrode. Figure 4 shows voltammograms obtained in potassium chloride (KCl) solutions at various concentrations. The voltage scan between the

working electrode and reference electrode was from -0.6 V to 0.6 V then back to -0.6 V at a scan rate of 0.24 V/sec.

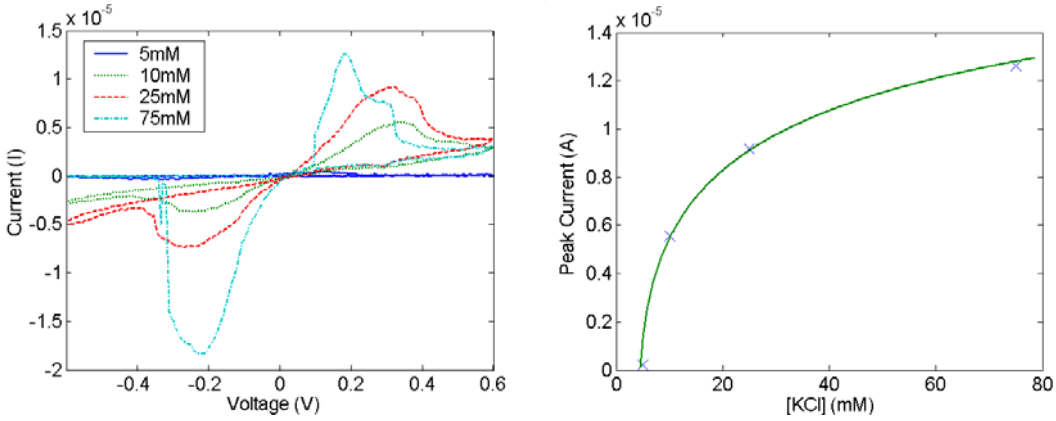

Figure 4. (a) Voltammogram for KCl solutions (b) Peak Current Response

The voltammogram shows the expected behavior for the reversible electrode reaction

$$2\,\mathrm{Cl}^- \leftrightarrow \mathrm{Cl}_2 + 2e^- . \qquad [5]$$

The forward peak current is monotonically dependent on the chloride concentration over the range 5 mM to 75 mM, as shown in Fig. 4(b). The peak current response tends toward saturation at higher concentrations. This may be a consequence of saturation of local Cl_2 concentration near the working electrode that obstructs the oxidation reaction (The solubility of chlorine gas in water is about 1 L per liter, which corresponds to about 45 mM Cl_2). The stability of the peak current at constant KCl concentration was tested by running one cycle of measurement every minute at a concentration of 25 mM. The observed peak current is stable within ±10% over times of 20 hours. However the corresponding potential for peak current response shifts as a function of KCl concentration. This suggests that the potential of the Ag/AgCl reference electrode changes when the Cl^- concentration changes, indicating that improvement in the reference electrode fabrication will be needed.

The lifetime of stable response is related to the degradation of the Ag/AgCl reference electrode. The reference electrode provides a stable potential through the reaction

$$\mathrm{AgCl}_{(s)} + e^- \leftrightarrow \mathrm{Ag}_{(s)} + \mathrm{Cl}^-, \quad E^\circ = 0.22V \qquad [6]$$

However, for AgCl in aqueous solution, there is also the solution/deposition equilibrium reaction

$$AgCl_{(s)} \leftrightarrow Ag^{+} + Cl^{-}, K_{sp} = 1.8 \times 10^{-10} \quad [7]$$

where K_{sp} refers to the solubility products (9). In cyclic voltammetry with a KCl solution, Cl^{-} is consumed during the oxidation half cycle, which disturbs the equilibrium and causes the dissolution of AgCl. During the reduction half cycle, Ag^{+} is deposited on the working electrode, which also causes the dissolution of AgCl. So during the entire cycle, AgCl is being dissolved. Eventually all of the AgCl is dissolved, and the reference electrode is no longer able to provide a stable potential.

V. Integrated Sensor Design

Figure 5 shows the layout of our integrated sensor design. There are three 3-electrode cells, each of which is controlled by a separate operational amplifier circuit. The potentiostat circuit is shown in Fig. 1. For testing purposes, three test operational amplifiers are also integrated on the chip. They are not connected with any electrodes, but with all the input terminals and output terminals externally accessible.

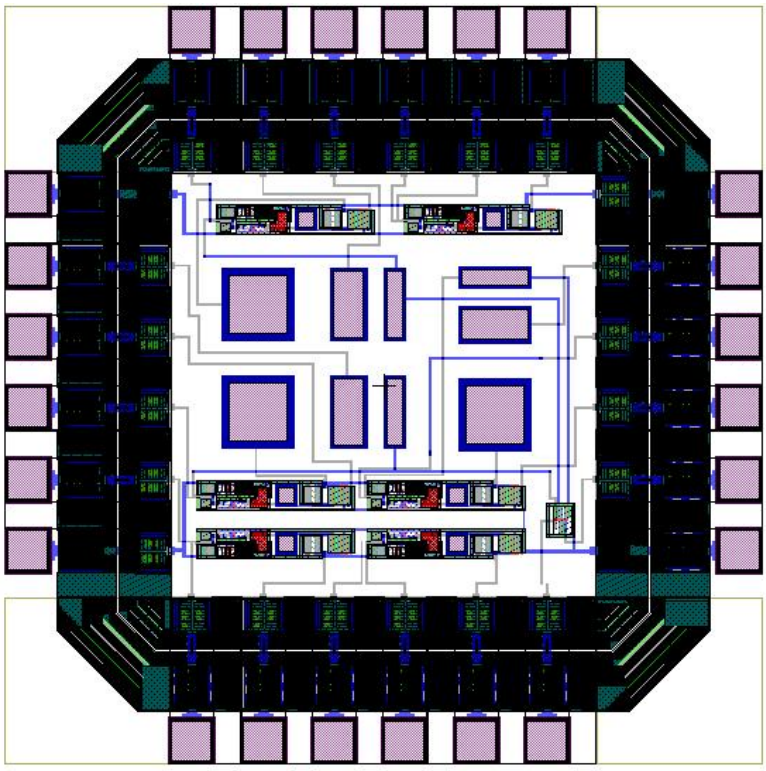

Figure 5. Chip Layout

A plating control circuitry is built using three NMOSFETs with W/L=30/3. The gates of these NMOSFET are connected together to the gate control terminal, and each NMOSFET connects with one reference electrode and with the plating terminal,

as shown in Fig. 6. We use the same positive and negative supply voltages V_{DD} and V_{SS} used for the operational amplifiers to turn the transistors on and off. When the gate terminal is connected to the +2.5V V_{DD} terminal, it turns the transistor on and allows plating current to pass. When the gate terminal is connected to the -2.5V V_{SS}, the transistor is turned off and external signals do not influence the sensor operation.

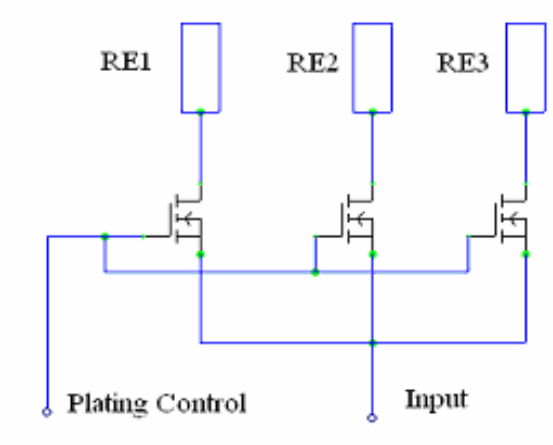

Figure 6. Plating Circuit

An important issue in the design of potentiostat circuits is the provision for measurement of the counter electrode current. Often this is done by measuring the voltage drop across an ungrounded series resistor (10); however this is not realistic on an integrated transducer. Consequently we designed an output circuit to externally measure the current response without disturbing the sensor operation. The circuit is shown in Fig. 7. The field effect transistors M2 and M6 mirror the current of M1 and M5. The current is measured by attaching a grounded external resistor R_{ext}. With equal W/L ratios for the transistors the counterelectrode current is given by $I = V_{ext}/R_{ext}$.

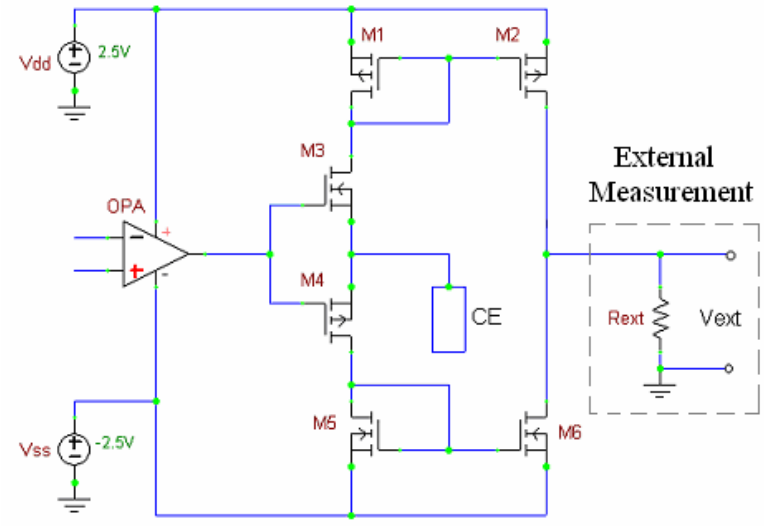

Figure 7. Output Circuit

VI. Conclusion

We have reported on progress toward developing an integrated chloride sensor based on cyclic voltammetry with microelectrodes. The process steps required to form the microelectrodes have been demonstrated and the completed electrodes have been tested. The sensitivity and stability of the 3-electrode sensor has been tested in KCl solutions with different concentrations and shows a good stable relation between the concentration and peak current response.

Acknowledgements

This work was supported by the Pennsylvania Infrastructure Technology Alliance and the National Science Foundation under Grant No. CMS-0329880. Any opinions, findings, and conclusions or recommendations expressed in this material are those of the authors and do not necessarily reflect the views of the National Science Foundation.

References

1. D.G.Watters, P.Jayaweera, A.J.Bahr, D.L.Huestis, N.Priyantha, R.Meline, *et al*, *Proeedings of SPIE,* **5057**, 20 (2003).
2. Halakatti Shekhar, V. Chathapuram, Seung H. Hyun, Seungkwan Hong, Hyoung J. Cho, *Proceedings of IEEE Sensors 2003*, **1**, 67 (2003).
3. Harpreet S. Narula, John G. Harris, *Proceedings of IEEE Computer Society Annual Symposium on VLSI 2004*, **1**, 268 (2004).
4. Feifei Cao, David W. Greve, I.J. Oppenheim, *IEEE Sensor 2005*, **1**, 195 (2005).
5. J. Wang, *Analytical Electrochemistry*, P. 129, Wiley-VCH, New York (2000).
6. MOSIS Integrated Circuit Fabrication Service, Marina del Rey, CA 90292
7. M. Datta, S.A. Merritt, and M. Dagenais, *IEEE Trans. Components and Packaging Technology*, **22**, 299 (1999).
8. Xiaoqiu Huang, I. Nausieda, David W. Greve, Michael M. Domach, Duc Nguyen, *Proceedings of IEEE Sensor 2004*, **1**, 72 (2004).
9. J.Koryta, *Principles of Electrochemistry*, P.70, John Wiley & Sons Ltd., West Sussex, England (1993).
10. Bank Elektronik- Intelligent Controls GmbH, Pohlheim, Germany.